J. Chem. Sci. Vol. 128, No. 5, May 2016, pp. 733–743. © Indian Academy of Sciences.
DOI 10.1007/s12039-016-1067-3

Kinetics and mechanism of uncatalyzed and ruthenium(III)-catalyzed oxidation of formamidine derivative by hexacyanoferrate(III) in aqueous alkaline medium

AHMED FAWZY[a,b]

[a]Chemistry Department, Faculty of Applied Sciences, Umm Al-Qura University, 21955 Makkah, Saudi Arabia
[b]Chemistry Department, Faculty of Science, Assiut University, 71516 Assiut, Egypt
e-mail: afsaad13@yahoo.com

MS received 4 January 2016; revised 17 February 2016; accepted 21 February 2016

Abstract. The catalytic effect of ruthenium(III) on the oxidation of *N*, *N*-dimethyl-*N*′-(4*H*-1,2,4-triazol-3-yl) formamidine (ATF) by hexacyanoferrate(III) (HCF) was studied spectrophotometrically in aqueous alkaline medium. Both uncatalyzed and catalyzed reactions showed first order kinetics with respect to [HCF], whereas the reaction orders with respect to [ATF] and [OH^-] were apparently less than unity over the concentration range studied. A first order dependence with respect to [Ru^{III}] was obtained. Increasing ionic strength increased the rate of uncatalyzed reaction and decreased the rate of the catalyzed one Plausible mechanistic schemes of oxidation reactions have been proposed. In both cases, the final oxidation products are identified as aminotriazole, dimethyl amine and carbon dioxide. The rate laws associated with the reaction mechanisms are derived. The reaction constants involved in the different steps of the mechanisms were calculated. The activation and thermodynamic parameters have been computed and discussed.

Keywords. Kinetics; mechanism; oxidation; ruthenium(III) catalysis; formamidine; hexacyanoferrate(III).

1. Introduction

Hexacyanoferrate(III) (HCF) is an efficient one-electron oxidant especially in alkaline media[1–5] due to its high stability, water solubility and its moderate reduction potential, 0.45 V, leading to its reduction to hexacyanoferrate(II), a stable product.[6] It adds less error to the experimental results, and the data can be analyzed meticulously to establish the reaction path.

Formamidines have achieved considerable importance in the last decades because of their biological activity.[7,8] The *N*, *N*-dialkyl derivatives are highly effective acaricides and the most rewarding of these studies resulted in the discovery of the acaricide insecticide chlordimeform. Oxidation of formamidines[9,10] is very important, since the *N*, *N*-dialkyl formamidine group is one of the most versatile protecting groups, especially in biosynthetic applications.[11] Formamidines form complexes with transition metal ions[12,13] and such complexes exhibit remarkable biological activity against certain microbes, viruses and tumors.[14,15] The presence of heteroatom in such ligands plays a key role when coordinated with these metal ions such as 1,2,4-triazole derivatives which act as bidentate ligands. Studies on ruthenium triazole complexes are scarce and limited to a few cases.[16–18] It is reported[16] that such complexes are the most promising complexes for anticancer chemotherapy (activity). Furthermore, transition metal ions are used as catalysts in various oxidation-reduction reactions because they have various oxidation states.[19–22]

Literature survey reveals that no work has been reported about the kinetics and mechanism of oxidation of ATF by HCF oxidant. This observation prompted me to investigate the title reactions. The aims of the present study were to establish the optimum conditions affecting oxidation of ATF by HCF in aqueous alkaline medium, to understand the active species of the reactants in such medium, to examine the catalytic activity of Ru^{III} catalyst and finally to elucidate plausible oxidation reaction mechanisms.

2. Experimental

2.1 *Materials*

The chemicals used in the present study were of reagent grade and their solutions were prepared by dissolving the requisite amounts of the samples in doubly distilled water. The solution of aminotriazole formamidine (ATF) was freshly prepared by dissolving the sample in dou-

bly distilled water. A solution of hexacyanoferrate(III) was prepared by dissolving potassium hexacyanoferrate(III) (BDH) in water and its concentration was ascertained by iodometric titration.[23(a)] Hexacyanoferrate(II) solution was obtained by dissolving potassium hexacyanoferrate(II) (S.D fine Chem.) in water and standardizing with cerium(IV) solution.[23(b)] The solution of ruthenium(III) chloride was prepared as described previously.[24] Sodium hydroxide and sodium perchlorate were used to vary the alkalinity and ionic strength, respectively.

2.2 *Kinetic measurements*

All kinetic runs were followed under pseudo-first order conditions with [ATF] »[HCF]. The progress of the uncatalyzed and Ru^{III}-catalyzed reactions was followed by measuring the decay of HCF absorbance as a function of time at its absorption maximum ($\lambda = 420$ nm), whereas the other constituents of the reaction mixtures do not absorb significantly at this wavelength. The absorbance measurements were made on a Shimadzu UV-VIS-NIR-3600 double-beam spectrophotometer.

The oxidation of ATF by HCF in alkaline medium was found to proceed with a slow rate in the absence of Ru^{III} catalyst and the catalyzed reaction is suggested to occur in parallel paths, with contributions from both catalyzed and uncatalyzed paths. Therefore, the total rate constant (k_T) is equal to the sum of the rate constants of the uncatalyzed (k_U) and catalyzed (k_C) reactions, so $k_C = k_T - k_U$. The rate constants were determined as the gradients of ln(absorbance) versus time plots. Average values of at least two independent runs of the rate constants were taken for the analysis. The rate constants were reproducible to within 4%.

3. Results and Discussion

3.1 *Time-resolved spectra*

The spectral scans during the oxidation of ATF by HCF in alkaline medium in the absence and presence of Ru^{III} catalyst are shown in figures 1a and 1b, respectively. In both cases, the scanned spectra indicate gradual decay of HCF(III) band with time as a result of its reduction to HCF(II). It can be observed that the decay of HCF at its absorption maximum during the catalyzed reaction is significantly faster than that of the uncatalyzed one. Furthermore, a careful examination of the spectral scans of the ruthenium(III)-catalyzed oxidation confirms growth of a new peak located at about 480 nm as shown in figures 2a,b with appearance of an isosbestic point at 465 nm suggesting formation of an intermediate complex between ATF and Ru^{III}.

3.2 *Stoichiometry and product analysis*

The stoichiometry was determined spectrophotometrically at $\lambda = 420$ nm at fixed alkalinity, ionic strength and temperature. The results indicate the consumption of two moles of HCF for one mole of ATF to yield the oxidation products as shown in the following scheme 1, where the compounds (I), (II) and (III) are ATF, aminotriazole and dimethyl amine, respectively. The above stoichiometric relation is consistent with the results of product analysis. The product, aminotriazole, was confirmed by spectral data. The IR spectrum showed the presence of two bands due to NH_2 group near 3415 and 3370 cm^{-1}. Dimethylamine was identified by spot test,[25] and carbon dioxide by lime water.

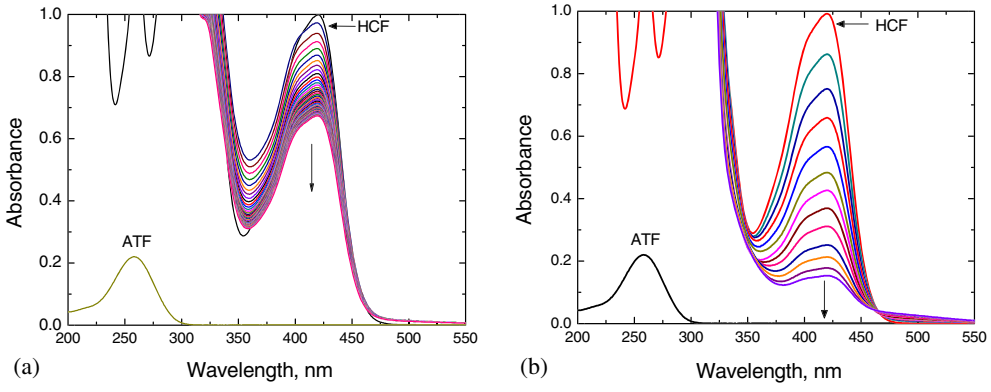

Figure 1. Time-resolved spectra for: (a) uncatalyzed, and (b) ruthenium(III)-catalyzed oxidation of ATF by HCF in alkaline medium. [ATF] = 0.03 mol dm^{-3}, [HCF] = 7.0×10^{-4} mol dm^{-3}, [OH^-] = 0.5 mol dm^{-3} and I = 1.0 mol dm^{-3} at 25°C. [Ru^{III}] = 5.0×10^{-6} mol dm^{-3}. Scan time intervals = 5 min.

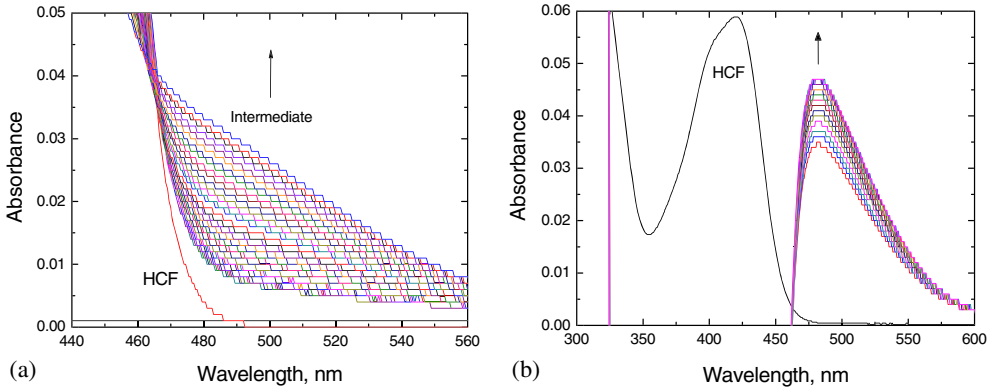

Figure 2. (a) Spectra taken from figure 1b, and b) New spectra where reference cell contains HCF and OH^- of the same reaction mixture concentrations.

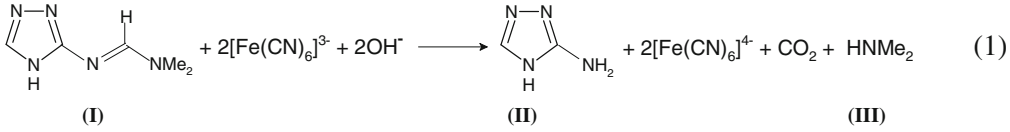

(1)

Scheme 1. Stoichiometric relation for the oxidation of ATF by HCF in alkaline medium.

3.3 *Order of reactions*

The orders of uncatalyzed and catalyzed reactions with respect to the reactants were determined from the slopes of the log k_U and log k_C versus log(concentration) plots by varying the concentrations of substrate, alkali and catalyst, in turn, while keeping other conditions constant.

Hexacynoferrate(III) oxidant was varied in both uncatalyzed and catalyzed reactions in the concentration range of 3.0×10^4 to 11.0×10^{-4} mol dm^{-3} while other variables such as the concentration of reductant, ruthenium(III) catalyst and sodium perchlorate were kept constant. The pH (13.7) and temperature were also kept constant. It has been observed that the increase in the oxidant concentration did not alter the oxidation rates of ATF (table 1). This indicates that the oxidation rates are independent of oxidant concentration and the order of reactions with respect to the oxidant is confirmed to be one.

The observed rate constants (k_U and k_C) were determined at different initial concentrations of the reductant ATF keeping others constant. The rates of both uncatalyzed and catalyzed reactions were found to increase with increasing [ATF] as listed in table 1. The orders with respect to [ATF] were found to be 0.79 and 0.71 for uncatalyzed and catalyzed reactions, respectively, as the slopes of plots of log k_U and log k_C versus log[ATF] (figure S1 in Supplementary Information).

The reaction rates were measured at constant [ATF], [HCF], [Ru^{III}] (for the catalyzed reaction), ionic strength and temperature but with various concentrations of the alkali ranging from 0.1 to 0.9 mol dm^{-3}. The rates of the reactions were found to increase with increasing [OH^-]. Plots of k_U and k_C versus [OH^-] were linear with positive intercepts (figure S2 in SI) confirming fractional-first order dependences with respect to [OH^-].

The ruthenium(III) catalyst concentration was varied from 1.0×10^{-6} to 9.0×10^{-6} mol dm^{-3} at constant [ATF], [HCF], [OH^-] and at constant ionic strength and temperature. Reaction rate was found to increase with increasing [Ru^{III}] (table 1). The order with respect to [Ru^{III}] was found to be unity as the slope of log k_C versus log[Ru^{III}] plot (figure S3 in SI).

3.4 *Effect of ionic strength*

The effect of ionic strength on both uncatalyzed and catalyzed reactions was studied by varying the $NaClO_4$ concentration. The rate of uncatalyzed reaction was found to increase with increasing ionic strength, whereas the rate of catalyzed reaction decreases with the increase of ionic strength. Thus, the plot of ln k_U and ln k_C versus $I^{1/2}/(1+I^{1/2})$ are linear with a positive slope for uncatalyzed path and with a negative slope for the catalyzed one as shown in figure 3.

Table 1. Effects of variation of [HCF], [ATF], [OH^-], [Ru^{III}] and ionic strength, I, on the observed first order rate constant values in the uncatalyzed and ruthenium(III)-catalyzed oxidation of ATF by HCF in alkaline medium at 25°C.

10^4[HCF] (mol dm^{-3})	10^2[ATF] (mol dm^{-3})	[OH^-] (mol dm^{-3})	10^6[Ru^{III}] (mol dm^{-3})	I (mol dm^{-3})	10^5 k_T(s^{-1})	10^5 k_U(s^{-1})	10^5 k_C(s^{-1})
3.0	3.0	0.5	5.0	1.0	90.4	17.9	72.5
5.0	3.0	0.5	5.0	1.0	91.8	18.2	73.6
7.0	3.0	0.5	5.0	1.0	91.5	18.1	73.4
9.0	3.0	0.5	5.0	1.0	92.1	18.7	73.4
11.0	3.0	0.5	5.0	1.0	90.7	17.1	73.6
7.0	1.0	0.5	5.0	1.0	41.1	8.1	33.1
7.0	2.0	0.5	5.0	1.0	68.6	13.9	54.6
7.0	3.0	0.5	5.0	1.0	91.5	18.1	73.4
7.0	4.0	0.5	5.0	1.0	108.5	24.3	84.5
7.0	5.0	0.5	5.0	1.0	134.2	28.8	105.2
7.0	3.0	0.1	5.0	1.0	31.5	5.2	26.3
7.0	3.0	0.3	5.0	1.0	59.8	10.9	48.9
7.0	3.0	0.5	5.0	1.0	91.5	18.0	73.4
7.0	3.0	0.7	5.0	1.0	116.8	25.2	91.6
7.0	3.0	0.9	5.0	1.0	141.7	31.3	110.4
7.0	3.0	0.5	1.0	1.0	37.8	18.1	19.7
7.0	3.0	0.5	3.0	1.0	61.7	18.1	43.6
7.0	3.0	0.5	5.0	1.0	91.5	18.1	73.4
7.0	3.0	0.5	7.0	1.0	126.3	18.1	108.2
7.0	3.0	0.5	9.0	1.0	157.8	18.1	139.7
7.0	3.0	0.5	5.0	1.0	91.5	18.1	73.4
7.0	3.0	0.5	5.0	1.2	88.4	19.2	69.2
7.0	3.0	0.5	5.0	1.5	85.1	21.4	63.7
7.0	3.0	0.5	5.0	1.7	80.2	23.0	57.2
7.0	3.0	0.5	5.0	2.0	74.4	24.5	49.9

Experimental error ±4%

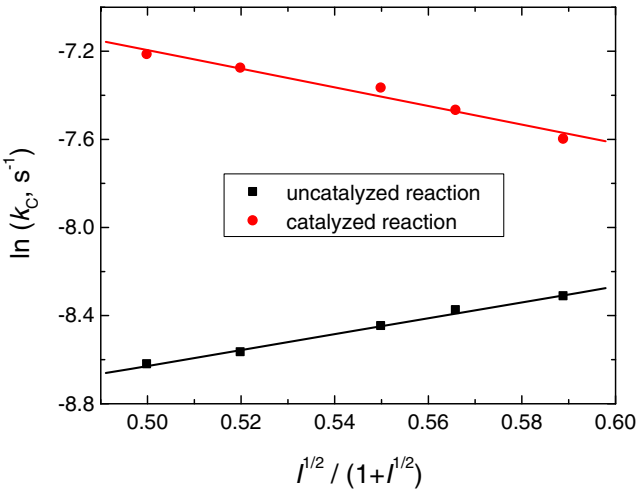

Figure 3. Debye-Huckel plots for the uncatalyzed and ruthenium(III)-catalyzed oxidation of ATF by HCF in alkaline medium. [ATF] = 0.03 mol dm^{-3}, [HCF] = 7.0×10^{-4} mol dm^{-3} and [OH^-] = 0.5 mol dm^{-3} at 25°C. [Ru^{III}] = 5.0×10^6 mol dm^{-3}.

3.5 *Effect of initially added product*

The effect of added hexacyanoferrate(II) product was studied also in the concentration range 3.0×10^{-4} to 11.0×10^{-4} mol dm^{-3} at fixed concentrations of the oxidant, reductant, alkali and catalyst. It was found that HCF(II) did not have any significant effect on the rates of reactions.

3.6 *Effect of temperature*

The rates of the uncatalyzed and ruthenium(III)-catalyzed reactions were measured at five different temperatures, namely, 288, 293, 298, 303 and 308 K under varying ATF, substrate and alkali concentrations. Both rates increased with the rise of temperature. The activation parameters of the rate constants of the slow steps of both uncatalyzed and ruthenium(III)-catalyzed reactions (k_1 and k_2) along with thermodynamic parameters of the equilibrium constants involved in the reaction mechanisms were evaluated and were listed in tables 3.

3.7 *Polymerization test*

The involvement of free radical species in the reactions was assayed by a polymerization test. A known quantity of acrylonitrile monomer was added to the reaction mixtures in an inert atmosphere, with the result of formation of white precipitates in the reaction mixtures suggesting presence of free radicals during reactions. When the experiments were repeated in the absence of ATF under similar conditions, the tests were negative. This indicates that the reactions proceeded through free radical paths.

3.8 *Mechanism of the uncatalyzed oxidation reaction*

HCF oxidation of ATF was found to occur in a slow rate in the absence of Ru^{III} catalyst in alkaline medium. The reaction has a stoichiometry of 2:1, *i.e.,* two moles of HCF consumed one mole of ATF. The reaction exhibits first order dependence with respect to [HCF] and less than unit order each with respect to both [ATF] and [OH^-]. The less than unit order in [OH^-] suggests deprotonation of ATF by the alkali in a pre-equilibrium step to form a more reactive species of the reductant. The rate is not significantly affected by HCF(II) suggesting absence of any fast equilibrium with the products in the rate-determining step. The latter should be irreversible as is generally the case for one-electron oxidants[26] and the oxidation takes place through generation of a free radical as obtained experimentally. The rate of reaction increases upon increasing the ionic strength of the medium suggesting that the reaction occurs between two similarly charged ions.[27,28]

On the other hand, the less than unit order in [ATF] suggests formation of a complex (C_1) between HCF and deprotonated ATF species which may be as a result of an outer sphere association through sodium cation bridge, *i.e.,* between ATF^- and $Na^+[Fe(CN)_6]^{3-}$ *i,e.,* $[NaFe(CN)_6]^{2-}$. Complex formation was proved kinetically by the non-zero intercept of the $1/k_U$ versus 1/[ATF] plot (figure 4) in favor of possible formation of an intermediate complex between the oxidant and substrate.[29] The formed complex (C_1) was slowly decomposed in the rate-determining step giving the initial oxidation products as the substrate radical ($ATF^{\cdot}$) and HCF(II). The substrate radical reacts with another HCF species in a subsequent fast step to yield an intermediate product, 1,1-dimethyl-2-hydroxy-3-(4*H*-1,2,4-triazol-3-yl) formamidine (or 1,1-dimethyl-3-(4*H*-1,2,4-triazol-3-yl) urea). In a further fast step, the intermediate product is hydrolyzed to give the final oxidation products as given in Scheme 2. Since scheme 2 is in accordance with the principle of non-complementary oxidations taking place in a sequence of one-electron steps, the reaction between ATF and HCF would afford a radical intermediate as obtained experimentally. Scheme 2 depicts the following equations:

The relationship between the reaction rate and the substrate, oxidant and alkali concentrations can be

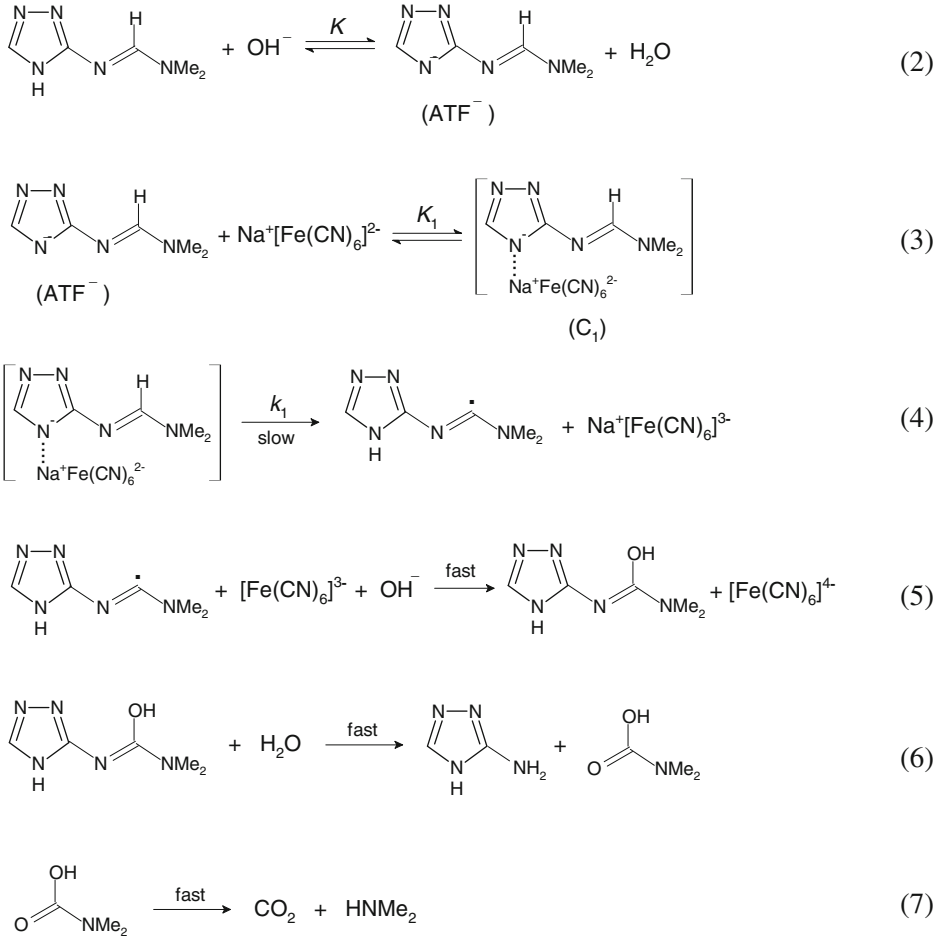

(2) (3) (4) (5) (6) (7)

Scheme 2. Mechanism of the uncatalyzed oxidation of ATF by HCF in alkaline medium.

Table 2. Values of the rate constants of the slow step (k_1) and the equilibrium constants (K and K_1) in the uncatalyzed oxidation of ATF by HCF in alkaline medium at different temperatures.

	Temperature (K)				
Constant	288	293	298	303	313
$10^4 k_1(s^{-1})$	3.11	4.88	6.51	9.30	11.69
$10^2 K(dm^3 mol^{-1})$	5.11	6.98	8.61	11.72	19.96
$10^{-2} K_1(dm^3 mol^{-1})$	4.87	4.21	3.38	2.44	1.15

Table 2a. Activation parameters associated with the slow step (k_1).

$\Delta S^{\neq}$ J mol^{-1}K^{-1}	$\Delta H^{\neq}$kJ mol^{-1}	$\Delta G^{\neq}_{298}$kJ mol^{-1}	$E^{\neq}_a$kJ mol^{-1}	A mol^{-1}s^{-1}
−131.31	56.14	95.27	58.64	2.17×10^5

Table 2b. Thermodynamic parameters associated with the equilibrium constants (K and K_1).

Equilibrium Constant	ΔH kJ mol^{-1}	ΔG_{298}kJ mol^{-1}	ΔS J mol^{-1}K^{-1}
K	40.95	6.08	117.01
K_1	−33.24	−14.43	−63.12

Experimental error ±4%.

deduced (see Appendix A) to give the following rate-law equation,

$$\text{Rate} = \frac{k_1 K K_1[\text{ATF}][\text{HCF}][\text{OH}^-]}{1 + K[\text{OH}^-] + K K_1[\text{ATF}][\text{OH}^-]} \quad (8)$$

The above rate law is consistent with all the observed orders with respect to different species. Under pseudo-first order condition, the rate-law can be expressed by Eq. (9),

$$\text{Rate} = \frac{-d[\text{HCF}]}{dt} = k_U[\text{HCF}] \quad (9)$$

Comparing Eqs. (8) and (9), the following relationship is obtained,

$$k_U = \frac{k_1 K K_1[\text{ATF}][\text{OH}^-]}{1 + K[\text{OH}^-] + K K_1[\text{ATF}][\text{OH}^-]} \quad (10)$$

Equation (9) can be verified by rearranging to Eqs. (11) and (12),

$$\frac{1}{k_U} = \left(\frac{1}{k_1 K K_1[\text{OH}^-]} + \frac{1}{k_1 K_1}\right)\frac{1}{[\text{ATF}]} + \frac{1}{k_1} \quad (11)$$

$$\frac{1}{k_U} = \left(\frac{1}{k_1 K K_1[\text{ATF}]}\right)\frac{1}{[\text{OH}^-]} + \frac{1}{k_1 K_1[\text{ATF}]} + \frac{1}{k_1} \quad (12)$$

Equations (11) and (12) require that plots of $1/k_U$ versus $1/[\text{ATF}]$ at constant $[\text{OH}^-]$, and $1/k_U$ versus $1/[\text{OH}^-]$ at constant [ATF] to be linear with positive intercepts and these are found to be so as shown in figures 4 and 5, respectively. The values of the rate constant of the slow step (k_1) at different temperatures obtained as reciprocal of the intercepts of $1/k_U$ versus 1/[ATF] plots are listed in table 2. The activation parameters of k_1 are calculated from the Arrhenius and Eyring plots and are listed in table 2a. Values of the equilibrium constants associated with the mechanistic scheme 2 (K and K_1) at different temperatures are calculated from the slopes and intercepts of such plots and are also inserted in table 2. The thermodynamic parameters of K and K_1 are evaluated from van't Hoff plots and these are also inserted in table 2b.

3.9 *Mechanism of ruthenium(III)-catalyzed oxidation reaction*

It was reported[30,31] that in alkaline solutions ruthenium(III) is mostly present as the hydroxylated species in the form of $[Ru(H_2O)_5OH]^{2+}$. The reaction between HCF and ATF in alkaline medium in the presence of traces of ruthenium(III) catalyst is similar to the uncatalyzed reaction with respect to stoichiometry and reaction orders. The reaction is first order with respect to ruthenium(III) catalyst. In the contrary to the uncatalyzed reaction, increasing ionic strength was found to decrease the rate. The observed less than unit order with respect to [ATF] presumably results from a complex formation between the substrate ATF and the catalyst ruthenium(III) in a pre-equilibrium step before the reaction with the oxidant. Spectral evidence for the complex formation was obtained from UV–Vis spectra

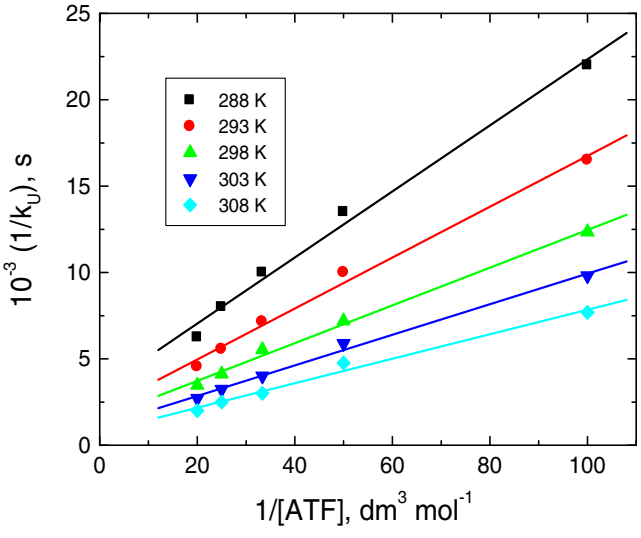

Figure 4. Plots of $1/k_U$ versus $1/[\text{ATF}]$ for the uncatalyzed oxidation of ATF by HCF in alkaline medium at different temperatures. $[\text{HCF}] = 7.0 \times 10^{-4}$ mol dm^{-3}, $[\text{OH}^-] = 0.5$ mol dm^{-3} and $I = 1.0$ mol dm^{-3}.

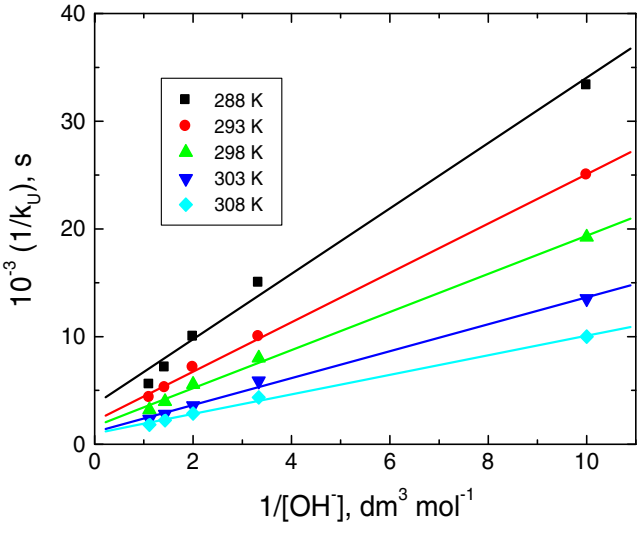

Figure 5. Plots of $1/k_U$ versus $1/[\text{OH}^-]$ for the uncatalyzed oxidation of ATF by HCF in alkaline medium at different temperatures. $[\text{HCF}] = 7.0 \times 10^{-4}$ mol dm^{-3}, [ATF] $= 0.03$ mol dm^{-3} and $I = 1.0$ mol dm^{-3}.

shown in figures 1b and 2a,b. The formation of the complex was also proved kinetically by a non-zero intercept of $[Ru^{III}]/k_C$ versus $1/[ATF]$ plot (figure 6).

In view of the above-mentioned aspects, deprotonated ATF is suggested to combine with Ru^{III} species, $[Ru(H_2O)_5OH]^{2+}$, to form an intermediate complex C_2 prior to the rate-determining step. Then, the oxidant HCF attack the formed complex in a slow (rate-determining) step to yield ATF free radical and HCF(II) with regeneration of the catalyst Ru^{III}. The radical intermediate reacts with another mole of the oxidant in a subsequent fast step to yield the final oxidation products. The results are accommodated in scheme 3.

The suggested mechanism leads to the following rate law expression,

$$\text{Rate} = \frac{k_2 K K_2[\text{ATF}][\text{HCF}][Ru^{III}][OH^-]}{1 + K[OH^-] + K K_2[\text{ATF}][OH^-]}) \quad (19)$$

Under pseudo-first order condition,

$$\text{Rate} = \frac{-d[\text{HCF}]}{dt} = k_C[\text{HCF}] \quad (20)$$

Therefore,

$$k_C = \frac{\text{Rate}}{[\text{HCF}]} = \frac{k_2 K K_2[\text{ATF}][Ru^{III}][OH^-]}{1+K[OH^-] + K K_2[\text{ATF}][OH^-]} \quad (21)$$

Equation (21) can be rearranged to the following forms, which are suitable for verification,

$$\frac{[Ru^{III}]}{k_C} = \left(\frac{1}{k_2 K K_2[OH^-]} + \frac{1}{k_2 K_2}\right)\frac{1}{[\text{ATF}]} + \frac{1}{k_2} \quad (22)$$

$$\frac{[Ru^{III}]}{k_C} = \left(\frac{1}{k_2 K K_2[\text{ATF}]}\right)\frac{1}{[OH^-]} + \frac{1}{k_2 K_2[\text{ATF}]} + \frac{1}{k_2} \quad (23)$$

Regarding Eqs. (22) and (23), plots of $[Ru^{III}]/k_C$ versus $1/[\text{ATF}]$ at constant $[OH^-]$ and $[Ru^{III}]/k_C$ versus $1/[OH^-]$ at constant [ATF] should be linear with positive intercepts. The experimental results satisfied these requirements as shown in figures 6 and 7, respectively. The values of the rate constant of the slow step (k_2) at different temperatures obtained as reciprocal of intercepts of $[Ru^{III}]/k_C$ versus $1/[\text{ATF}]$ plots are listed in table 3. The activation parameters of k_2 are calculated and are inserted in table 3a. Also, the plots of $[Ru^{III}]/k_C$ versus $1/[OH^-]$ yield straight lines with

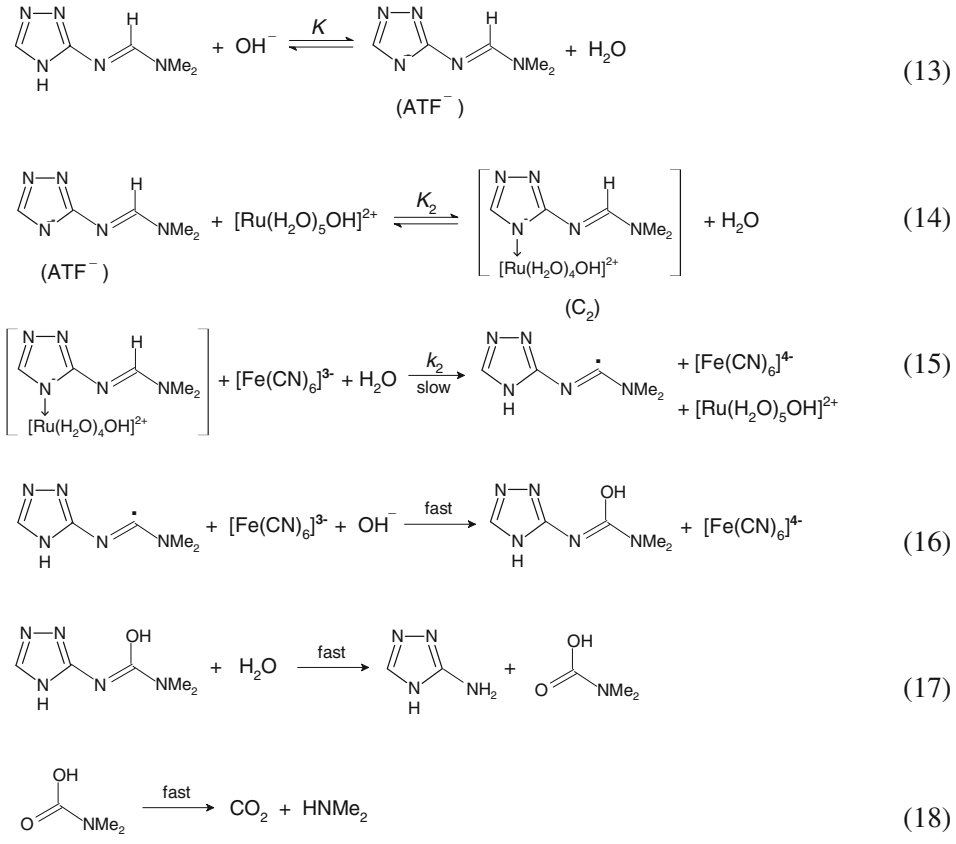

(13) (14) (15) (16) (17) (18)

Scheme 3. Mechanism of ruthenium(III)-catalyzed oxidation of ATF by HCF in alkaline medium.

their slopes and intercepts equal to $1/k_2KK_2$[ATF] and $1/k_2K_2$[ATF]+$1/k_2$, respectively Thus, the values of the equilibrium constants associated with the mechanistic scheme 3 (K and K_2) at different temperatures as well as their thermodynamic parameters of K and K_2 are evaluated and are also listed in table 3b.

The obtained large negative values of $\Delta S^{\neq}$ (listed in tables 2 and 3) suggest compactness of the formed complexes and such complexes are more ordered than the reactants due to loss of degrees of freedom.[32] Also, the obtained values of $\Delta S^{\neq}$ are within the range of radical reactions.

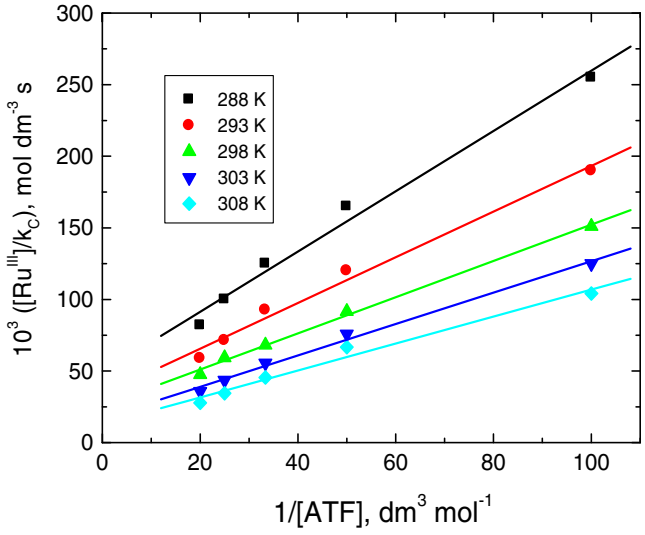

Figure 6. Plots of $[Ru^{III}]/k_C$ versus 1/[ATF] for the ruthenium(III)-catalyzed oxidation of ATF by HCF in alkaline medium at different temperatures. [HCF] = 7.0×10^{-4} mol dm^{-3}, [OH$^-$] = 0.5 mol dm^{-3} and I = 1.0 mol dm^{-3}.

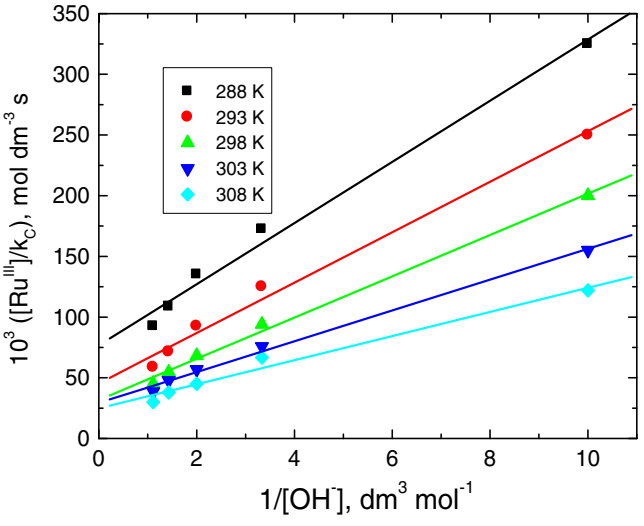

Figure 7. Plots of $[Ru^{III}]/k_C$ versus 1/[OH$^-$] for the ruthenium(III)-catalyzed oxidation of ATF by HCF in alkaline medium at different temperatures. [HCF] = 7.0×10^{-4} mol dm^{-3}, [ATF] = 0.03 mol dm^{-3} and I = 1.0 mol dm^{-3}.

Table 3. Values of the rate constants of the slow step (k_2) and the equilibrium constants (K and K_2) in the ruthenium(III)-catalyzed oxidation of ATF by HCF in alkaline medium at different temperatures.

	Temperature (K)				
Constant	288	293	298	303	313
k_2(s^{-1})	19.97	31.31	43.17	57.89	73.74
10^2K(dm^{3}mol^{-1})	6.74	7.99	10.09	11.97	15.88
$10^{-2}K_2$(dm^{3}mol^{-1})	8.44	7.27	6.11	4.36	2.28

Table 3a. Activation parameters associated with the slow step (k_2).

$\Delta S^{\neq}$J mol^{-1}K^{-1}	$\Delta H^{\neq}$kJ mol^{-1}	$\Delta G^{\neq}_{298}$kJ mol^{-1}	$E^{\neq}_a$kJ mol^{-1}	A mol^{-1}s^{-1}
−62.21	42.20	60.73	43.69	9.71×10^9

Table 3b. Thermodynamic parameters associated with the equilibrium constants (K and K_2).

Equilibrium Constant	ΔH^okJ mol^{-1}	ΔG^o_{298}kJ mol^{-1}	ΔS^oJ mol^{-1}K^{-1}
K	31.19	5.70	85.54
K_2	−31.18	−15.89	−51.29

Experimental error ±4%.

4. Conclusions

The reaction between *N*, *N*-dimethyl-*N*′-(4*H*-1,2,4-triazol-3-yl) formamidine and hexacyanoferrate(III) in alkaline medium was found to proceed with a slow rate in the absence of Ru^{III} catalyst. Plausible mechanistic schemes of oxidation reactions in the absence and presence of the catalyst have been proposed. The final oxidation products are identified as aminotriazole, dimethyl amine and carbon dioxide.

Supplementary Information (SI)

All additional information pertaining to the order with respect to substrate (figure S1), alkali (figure S2) and catalyst (figure S3) are given in the supporting information, available at www.ias.ac.in/chemsci.

Appendix A. Derivation of the rate-law expression for the uncatalyzed oxidation reaction.

According to the suggested mechanistic scheme 2,

$$\text{Rate} = \frac{-d[\text{HCF}]}{dt} = k_1[\text{C}_1] \tag{A1}$$

$$\text{K} = \frac{[\text{ATF}^-]}{[\text{ATF}][\text{OH}^-]}, [\text{ATF}^-] = K[\text{ATF}][\text{OH}^-] \tag{A2}$$

$$K_1 = \frac{[\text{C}_1]}{[\text{ATF}^-][\text{HCF}]}, [\text{C}_1] = K_1[\text{ATF}^-][HCF] = KK_1[\text{ATF}][\text{HCF}][\text{OH}^-] \tag{A3}$$

Substituting Eq. (A3) into Eq. (A1) leads to,

$$\text{Rate} = k_1 K K_1[\text{ATF}][\text{HCF}][\text{OH}^-] \tag{A4}$$

The total concentration of ATF is given by,

$$[\text{ATF}]_\text{T} = [\text{ATF}]_\text{F} + [\text{ATF}^-] + [\text{C}_1] \tag{A5}$$

$$[\text{ATF}]_\text{F} = \frac{[\text{ATF}]_\text{T}}{1 + K[\text{OH}^-] + KK_1[\text{HCF}][\text{OH}^-]} \tag{A6}$$

In view of low [HCF], the third denominator term KK_1[HCF][OH] in the above equation can be neglected. Therefore, Eq. (A6) can be simplified to the following equation,

$$[\text{ATF}]_\text{F} = \frac{[\text{ATF}]_\text{T}}{1 + K[\text{OH}^-]} \tag{A7}$$

$$[\text{HCF}]_\text{T} = [\text{HCF}]_\text{F} + [\text{C}_1] \tag{A8}$$

$$[\text{HCF}]_\text{F} = \frac{[\text{HCF}]_\text{T}}{1 + KK_1[\text{ATF}][\text{OH}^-]} \tag{A9}$$

Substituting Eqs. (A7) and (A9) into Eq. (A4) (and omitting 'T' and 'F' subscripts) leads to,

$$\text{Rate} = \frac{k_1 K K_1[\text{ATF}][\text{HCF}][\text{OH}^-]}{(1 + K[\text{OH}^-])(1 + KK_1[\text{ATF}][\text{OH}^-])} \tag{A10}$$

Under pseudo-first order condition, the rate-law can be expressed by Eq. (A11),

$$\text{Rate} = \frac{-d[\text{HCF}]}{dt} = k_\text{U}[\text{HCF}] \tag{A11}$$

Comparing Eqs. (A10) and (A11), the following relationship is obtained.

$$k_\text{U} = \frac{k_1 K K_1[\text{ATF}][\text{OH}^-]}{1 + K[\text{OH}^-] + KK_1[\text{ATF}][\text{OH}^-] + K^2K_1[\text{ATF}][\text{OH}^-]^2} \tag{A12}$$

The term $K^2K_1[\text{ATF}][\text{OH}^-]^2$ in the denominator of Eq. (A12) is negligibly small compared to unity in view of the low concentration of ATF used. Therefore, this term can be deleted and with rearrangement, the following equations are obtained.

$$\frac{1}{k_\text{U}} = \left(\frac{1}{k_1 K K_1[\text{OH}^-]} + \frac{1}{k_1 K_1}\right)\frac{1}{[\text{ATF}]} + \frac{1}{k_1} \tag{A13}$$

$$\frac{1}{k_\text{U}} = \left(\frac{1}{k_1 K K_1[\text{ATF}]}\right)\frac{1}{[\text{OH}^-]} + \frac{1}{k_1 K_1[\text{ATF}]} + \frac{1}{k_1} \tag{A14}$$

References

1. Devra V and Yadav M B 2012 *Russ. J. Chem.* **5** 67
2. Shukla R and Upadhyay S K 2008 *Indian J. Chem.* **47A** 551
3. Jose T P, Nandibewoor S T and Tuwar S M 2006 *J. Sulfur Chem.* **27** 25
4. Kelson E P and Phengsy P P 2000 *Int. J. Chem. Kinet.* **32** 760
5. Leal J M, Garcia B and Domingo P L 1998 *Coord. Chem. Rev.* **173** 79
6. Farokhi S A and Nandibewoor S T 2003 *Tetrahedron* **59** 7595
7. (a) Beeman R W and Matsumura F 1973 *Nature* **242** 273; (b) Aziz S A and Knowles C O *Nature* **242** 417
8. Leung V S K, Chan T Y K and Yeung V T F 1999 *Clin. Toxicol.* **37** 513
9. Fawzy A and Shaaban M R 2014 *Transition Met. Chem.* **39** 379
10. Asghar B H and Fawzy A 2014 *J. Saudi. Chem. Soc.* doi: 10.1016/j.jscs.2014.12.001
11. Goel A and Sharma S 2010 *Transition Met. Chem.* **35** 549
12. Meyers A I and Hutchings R 1996 *Heterocycles* **42** 475
13. Matulenko M and Meyers A I 1996 *J. Org. Chem.* **61** 573
14. Padhye S and Kaufman G B 1985 *Coord. Chem. Rev.* **63** 127

15. Asiri A M and Khan S A 2010 *Molecules* **15** 4784
16. Groessl M, Reisner E, Hartinger C G, Eichinger E, Semenova O, Timerbaev A R, Jakupec M A, Arion V B and Keppler B K 2007 *J. Med. Chem.* **50** 2185
17. Jha A, Murthy Y L N, Durga G and Sundari T T 2010 *E-J. Chem.* **7** 1571
18. Asiri A M, Baghlaf A O, Abdel-Rahman R M, Khan S A and Ishaq M 2013 *Asian J. Chem.* **25** 7779
19. Das A K 2001 *Coord. Chem. Rev.* **213** 307
20. Fawzy A 2015 *Int. J. Chem. Kinet.* **47** 1
21. Fawzy A 2014 *Transition Met. Chem.* **39** 567
22. Fawzy A 2015 *Transition Met. Chem.* **40** 287
23. Jeffery G H, Bassett J, Mendham J and Denney R C 1996 In *Vogel's text book of quantitative chemical analysis* 5th edn (ELBS Longman: Essex) (a) p. 399 and (b) p. 384
24. Puttaswamy R and Jagadeesh R V 2005 *Appl. Catal. A* **292** 259
25. Feigl F 1975 In *Spot tests in organic analysis* (New York: Elsevier) p. 195
26. Leal J M, Domingo P L, Garcla B and Ibeas S 1993 *J. Chem. Soc. Faraday Trans.* **89** 3571
27. Frost A A and Person R G 1970 In *Kinetics and mechanism* (New Delhi: Wiley Eastern) p. 147
28. Amis E S 1966 In *Solvent effect on reaction rates and mechanism* (Academic Press: New York) p. 28
29. Michaelis L and Menten M L 1918 *Biochem. Z.* **49** 333
30. Mech M D, Meti K S, Byadagi, Nandibewoor S T and Chimatadar S A 2014 *Monatsh. Chem.* **145** 1561
31. Chimatadar S A, Kini A K and Nandibewoor S T 2005 *Inorg. React. Mech.* **5** 231
32. Weissberger A 1974 In *Investigation of rates and mechanism of reactions in techniques of chemistry* (New York: Interscience Publication) p. 421